Towards Spatio-Spectral analysis of Sentinel-2 Time Series data for land cover mapping

Yawogan Jean Eudes Gbodjo, Dino Ienco and Louise Leroux

***Abstract*—Modern Earth Observation (EO) systems produce huge volumes of images with the objective to monitor Earth surface. Due to the high revisit time of EO systems such the Sentinel-2 constellation, satellite image time series (SITS) are continuously produced allowing to improve the monitoring of spatio-temporal phenomena. How to efficiently analyze SITS considering both spectral and spatial information is still an open question in the remote sensing field. To deal with SITS classification, in this letter we propose a spatio-spectral classification framework that leverages mathematical morphology to extract spatial characteristics from SITS data and combines them with the already available spectral and temporal information. Experiments carried out on two study sites characterized by different heterogeneous land cover have demonstrated the significance of our proposal and the value to combine spatial as well as spectral information in the context of SITS land cover classification.**

***Index Terms*—Satellite Image Time Series, Mathematical Morphology, Land Cover classification, Sentinel-2**

I. Introduction

NOWADAYS, modern Earth Observation programs, supported by national or continental spatial missions, provide massive volume of remote sensing data every day. Among such programs, a notable example is the Copernicus programme, supported by the European Spatial Agency (ESA). In the Copernicus programme, the Sentinel-2 (S2) mission involves a constellation of two satellites with a spatial resolution of 10-m and 20/60-m, a targeted revisit time of 5-days supplying optical information ranging from visible to near and shortwave infrared [1]. The unprecedented spatial and temporal resolutions offered by the S2 mission permits to generate dense Satellite Images Time Series (SITS).

Such data is becoming a valuable source of information for a wide range of land monitoring applications: agricultural management [2], [3], fire mapping [4] and vegetation growth [5] tasks. Among the different tasks, S2 data is getting more and more attention to cope with Land Use/Land Cover (LULC) mapping [6], [7] taking advantage of the spectral dynamics they carrying out.

Despite the fact that SITS allows to leverage spectral-temporal dynamics, that are essential to characterize certain LULC types [8], some land cover classes (e.g. urban areas or some agricultural land cover classes) are also characterized by particular spatial patterns that standard pixel-based analyses (e.g. [6], [9]) are not able to exploit. In the general field of remote sensing analysis, spatio-spectral classification has already demonstrated its usefulness mainly for hyperspectral [10] and multispectral [11] mono-temporal image analyses. Such strategies integrate the already available spectral information with spatial contextual features extracted via Mathematical Morphology [12], [13], a theory and technique used to analyze spatial relationships among pixels. More precisely, several morphological operators at different scales are applied to an image to derive multi-resolution representations. The derived Morphological Profiles (MPs) are then used, jointly with the input images, like a new set of features for the subsequent classification task. Relying on previous spatio-spectral classification frameworks commonly exploited in the remote sensing field for the analyses of mono-temporal images [10], [11], [14], here, we propose to exploit spatio-spectral analysis to enhance the land cover mapping task from S2 time series data. More in detail, the core idea of this study relies on the extraction of the spatial characteristics from SITS data via morphological operators at different spatial scales and, successively, the combination of such features with the already available time series spectral information. Such a process permits to inject spatial knowledge in the land cover mapping process involving the SITS data. To the best of our knowledge, this is the first work towards proposing a framework to integrate spatial contextual information, under the form of morphological profiles, with spectral/temporal features for the classification of optical (S2) SITS data.

II. Data Description

The analysis was carried out on the *Reunion Island* study site, a french overseas department located in the Indian Ocean and on a part of the *Dordogne* department in the southwest of France. The *Reunion Island* dataset consists of a time series of 21 S2 images acquired between January and December 2017 while the *Dordogne* dataset consists of a time series of 23 S2 images acquired between January and December 2016. The spatial extent of the *Reunion Island* site is $6\,666 \times 5\,916$ pixels while the extent for the *Dordogne* site is $5\,578 \times 5\,396$ pixels. All the S2 images used are those provided at level 2A (top of canopy reflectance) by the THEIA pole [1] and contain less than 50% of cloudy pixels. Only 10-m spatial resolution bands were used i.e. Blue, Green, Red, and Near Infrared (resp. B2, B3, B4, and B8). A temporal gap-filling [6] was performed to replace cloudy observations over each band using the previous and following cloud-free dates and the Normalized Difference

Y. JE. Gbodjo is with IRSTEA, UMR TETIS, University of Montpellier, Montpellier, France (email: jean-eudes.gbodjo@irstea.fr)

D. Ienco is with IRSTEA, UMR TETIS, LIRMM, University of Montpellier, Montpellier, France (email: dino.ienco@irstea.fr)

L. Leroux is with Cirad, UPR AÏDA, Dakar, Sénégal and AÏDA, Univ Montpellier, Cirad, Montpellier, France (email: louise.leroux@cirad.fr)

[1] http://theia.cnes.fr

Vegetation Index (NDVI) [15] was calculated for each date. The reference database including labeled samples with land cover classes for the *Reunion Island* was built from various sources : the Registre Parcellaire Graphique (RPG) [2] reference data for 2014, GPS land cover records from June 2017 completed by expert-knowledge based on visual interpretation of a SPOT6/7 to distinguish natural and urban areas. For the *Dordogne* site, the reference database was built from RPG reference data for 2016 and visual interpretation of a SPOT6/7 image as well. Finally, the ground truth databases (available in GIS vector format as a collection of class attributed polygons which have been converted to raster format at the S2 spatial resolution of 10-m) included 6 265 objects (880 775 pixels) over 11 classes for the *Reunion Island* and 3 819 objects (816 842 pixels) over 7 classes for the *Dordogne* site. The characteristics of the reference data for the *Reunion Island* and *Dordogne* are reported in Table I and Table II, respectively.

TABLE I
CHARACTERISTICS OF THE REUNION ISLAND GROUND TRUTH

Class	Label	Objects	Pixels
1	*Sugar cane*	869	89030
2	*Pasture and fodder*	582	68180
3	*Market gardening*	758	17578
4	*Greenhouse crops or Shadows*	260	1934
5	*Orchards*	767	33675
6	*Wooded areas*	570	204928
7	*Moor and Savannah*	506	155263
8	*Rocks and natural bare soil*	299	154284
9	*Shadows due to relief*	81	54336
10	*Water*	177	82584
11	*Urbanized areas*	1396	18983

TABLE II
CHARACTERISTICS OF THE DORDOGNE SITE GROUND TRUTH

Class	Label	Objects	Pixels
1	*Urbanized areas*	800	2105
2	*Crops*	600	94026
3	*Water*	800	50704
4	*Forest*	200	379910
5	*Moor*	187	99861
6	*Orchards*	632	97557
7	*Vines*	600	97557

III. SITS SPATIO-SPECTRAL CLASSIFICATION VIA MATHEMATICAL MORPHOLOGY

In this section, the spatio-spectral framework for SITS data is presented. Figure 1 depicts the proposed workflow.

Firstly, given a S2 time series dataset, like the ones described in Section II, composed of the five bands time series (i.e. B2, B3, B4, B8 and NDVI); a per-band principal component analysis (PCA) was applied. For each band time series, the m principal components (PC) corresponding to 99% of the cumulative variance were retained. The 99% threshold is commonly used in order to reduce data redundancy while keeping as much as possible the underlying variation [14]. Subsequently, several mathematical morphology (MM) operators [13] are applied to each of the PC.

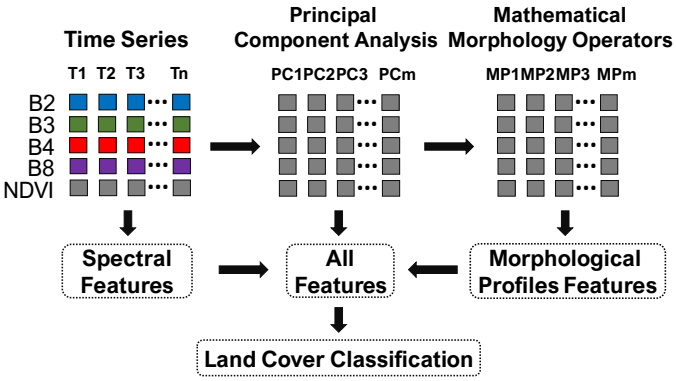

Fig. 1. Visual representation of the workflow. Firstly, the principal components for each band time series were derived, then multi-resolution morphological operators were applied to obtain spatial features and finally, spatial and spectral features were combined to perform the land cover mapping.

MM allows extracting useful features which can describe the spatial patterns present in the image based on different operators [16]. Fundamentals operators in MM are *erosion* and *dilation* [13]. These operators are applied to an image using a Structuring Element (SE) to consider the spatial neighborhood around a pixel. The *erosion* operator shrinks objects that fit the shape of SE, while the *dilation* operator expands them [17]. Other operators in MM are *opening* and *closing* which are combinations of the first two operators. The dilation of an eroded image is known as *opening* and, conversely, the erosion of a dilated image is known as *closing*. An overview of these operators can be found in [13], [18]. Furthermore, the different operators can be applied at different spatial scales aiming at capturing multi-resolution spatial information considering the neighborhood of a pixel. In this study, a disk SE with a radii ranges in the set of values $\{3,5,7\}$ and four different operators: $\{$*erosion*, *dilation*, *opening*, *closing*$\}$ were considered. Yet, a total of 12 morphological operations were applied to each principal component previously derived. Specifically, for each pixel i of an arbitrary principal component, a feature set of size 12 (the number of morphological operations we have considered) plus 1 (the principal component value) were obtained. Due to the fact that m principal components have been retained for a specific band time series, a generic pixel will be described by a vector of $13 \times m \times 5$ values (the number of bands contained in the original optical SITS data) in the morphological profiles. The four aforementioned operators, at different scale resolution, were obtained via the *OrfeoToolBox* [3] employing the *GrayScale Morphological Operation* application using the disk as structuring element with varying radii in the range previously reported. Hereafter, the features extracted by morphological operators are named *morphological profile features*.

[2]RPG is part of the European Land Parcel Identification System (LPIS), provided by the French Agency for services and payment

[3]https://www.orfeo-toolbox.org/

IV. Experiments

In this section, the quality of the spatio-spectral classification framework is assessed with respect to competitors on the study sites introduced in Section II. Specifically, the joint use of morphological profiles (MPs) and the original spectral features (SF) coupled with the Random Forest (RF) classifier was applied and named *RF(SF,MPs)*. As competitors, a RF classifier using only spectral features (resp. principal components and morphological profile features) was tested and named *RF(SF)* (resp. *RF(PCs)* and *RF(MPs)*). The number of features for each classification scheme and study area can be found in Table III. We firstly report and discuss the average results for each study site. Then, a per-class analysis is provided and finally map details produced on the *Reunion Island* via the different competing methods are visually inspected.

TABLE III
Number of features for each representation: Spectral Features (SF), Principal Components (PC) and Morphological Profiles (MP) involved in the proposed workflow over the two study sites

Time series	Reunion site			Dordogne site		
	SF	PC	MP	SF	PC	MP
B2	21	17	221	23	18	234
B3	21	17	221	23	17	221
B4	21	17	221	23	16	208
B8	21	11	143	23	17	221
NDVI	21	16	208	23	18	234
Total	**105**	**78**	**1014**	**115**	**86**	**1118**

A. Experimental settings

For each study site, a train, validation, and test split with an object proportion of 50%, 20%, and 30%, respectively, was considered. Similarly to [6], pixels of the same objects were imposed to belong exclusively to the train, test or validation set avoiding a possible spatial bias in the evaluation procedure. The validation set was used to optimize the selection of the models hyper-parameters via a grid search procedure on the number of trees as well as the maximum depth of each tree. The former varies in the range $\{200,300,400,500\}$ while the latter spans over the range $\{20,40,60,80,\infty\}$. The model with the best hyper-parameters was then used to classify the test set. The assessment of the classification was done considering the overall *Accuracy*, the *Kappa* coefficient and the *F1* score [19]. Since the performances of the models may vary depending on the split of the data due to simpler or more complex samples involved in the training/test set, all assessment metrics are averaged over five iterations of different random splits following the strategy previously reported.

B. Results and Discussions

Table IV report the average results of different classification schemes on the *Reunion Island* and the *Dordogne* benchmark, respectively. Regarding average behaviors, the RF classifiers involving MPs features achieve better performances than the classifiers trained on the original SF or the derived PC for both of the study sites. Overall, *RF(MPs)* gains one point (resp. two points) on the *Reunion Island* (resp. *Dordogne*) study site. Furthermore, the RF classifier that involves the concatenation of all of the features, i.e. *RF(SF,MPs)*, outperforms the other competitors. The union of the original spectral features with the morphological profile features slightly improves the classification performance rather than using morphological profile features only. On the other hand, the RF classifier that involves only the PCs performs the worst on the two study sites. This is not surprising since we lost a bit of the temporal information via the reduction process. In addition, manual investigations of the feature importance supplied as side information from the *RF(SF,MPs)* model were conducted. MPs features are located in top positions of the rank indicating that such information is effective in the decision process of the classifier.

Figure 2a and Figure 2b show the averaged per-class F1 score obtained by each competing methods on the *Reunion Island* and *Dordogne* study site, respectively. Overall,

TABLE IV
Averaged F1 score, Kappa and Accuracy considering the different RF approaches (RF(SF), RF(PCs), RF(MPs), RF(SF,MPs)) on the two study sites

Classifier	Reunion site			Dordogne site		
	F1	Kappa	Acc.	F1	Kappa	Acc.
RF(SF)	0,884	0,861	0,884	0,849	0,786	0,853
RF(PCs)	0,851	0,824	0,853	0,840	0,774	0,846
RF(MPs)	0,893	0,873	0,894	0,860	0,806	0,868
RF(SF,MPs)	**0,901**	**0,883**	**0,902**	**0,863**	**0,809**	**0,869**

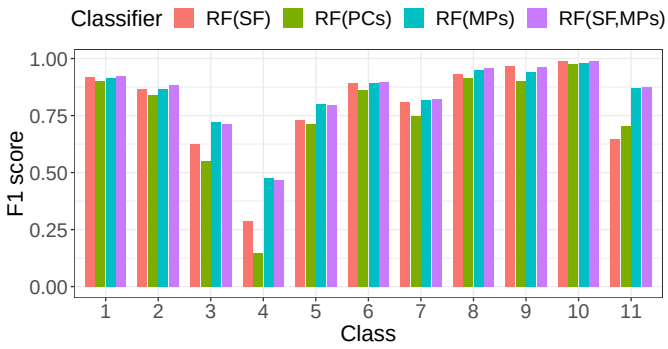

(a) *Reunion site*

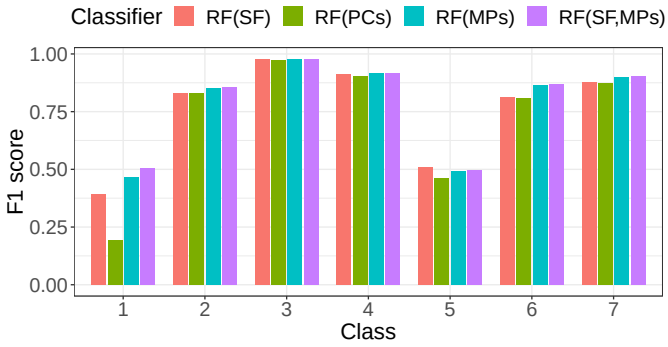

(b) *Dordogne site*

Fig. 2. Averaged per-class F1 score of the different RF approaches (RF(SF), RF(PCs), RF(MPs), RF(SF,MPs)) on the two study sites, see Tables I and II for class definition.

RF(SF,MPs) achieves the best score on seven classes over eleven for the *Reunion Island* while it is the best classifier on five classes over seven for the *Dordogne* site. Considering all the other classes, *RF(SF,MPs)* obtains very similar (or comparable) behavior with respect to the competitors. More precisely, considering the *Reunion Island* study site the results on classes: 3-*Market gardening*, 4-*Greenhouse crops or Shadows*, 5-*Orchards* and 11-*Urbanized areas* are sensibly improved while the biggest improvements on the *Dordogne* site are related to the classes: 1-*Urbanized areas* and 6-*Orchards*. This suggests that urban and agricultural land cover types are characterized by a spatial pattern which is, logically, better described by information coming from morphological profiles features. Considering *RF(PCs)*, we note that the dimensionality reduction seriously influences the classification behavior.

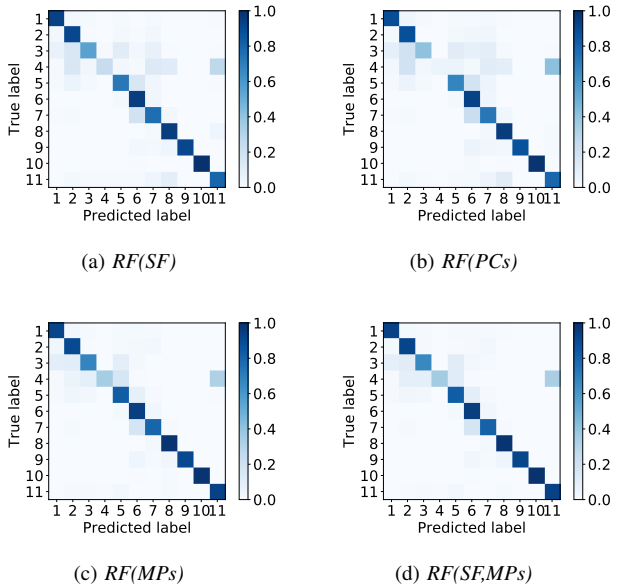

(a) *RF(SF)* (b) *RF(PCs)*

(c) *RF(MPs)* (d) *RF(SF,MPs)*

Fig. 3. Confusion Matrices for the Reunion Island study site considering the different RF approaches: *RF(SF)*, *RF(PCs)*, *RF(MPs)*, *RF(SF,MPs)*.

To better understand the misclassification behavior of the different competitors, the confusion matrices obtained by the different methods are investigated. Due to space limitation, only matrices and discussions for the *Reunion Island* study site are reported here since the *Reunion Island* exhibits a more heterogeneous and challenging landscape in terms of land cover classes than the *Dordogne*. The confusion matrices are reported in Figure 3. These confusion matrices are produced with the model that achieves the best *Accuracy* performances over the five iterations. We can notice that all the methods make some confusion on classes: 3-*Market gardening*, 4-*Greenhouse crops or Shadows* and 5-*Orchards*. Considering the class 3-*Market gardening*, some confusions appear with classes 2-*Pasture and fodder* and 5-*Orchards*. This behavior is more evident for the *RF(PCs)* and *RF(SF)* classifiers while it is alleviated for the classifiers *RF(MPs)* and *RF(SF,MPs)* due to the introduction of spatial information via morphological profile features. This can be related to the fact that such classes are characterized by particular spatial patterns that can be leveraged using contextual information coming from neighborhood pixels (e.g. regular trees plantation for orchards). Regarding the 4-*Greenhouse crops or Shadows* class, all the methods make confusion on this land cover type with the main confusion between it and class 11-*Urbanized areas*. Also in this case, the use of morphological profile features supports a better detection of such class. Notice that these classes represent land cover types that have very similar temporal radiometric behaviors but they can be characterized by different spatial contexts.

Finally, Figure 4 reports two representative map details of the *Reunion Island* corresponding to the classification produced by *RF(SF)* and *RF(SF,MPs)* competing methods. The first detail (Fig. 4a, 4b and 4c) focuses mainly on a mixed urban and agricultural area. In the *RF(SF)* classification, a salt and pepper effect can be highlighted over urban areas which result in confusion with 8-*Rocks and natural bare soils* class. On the other hand, *RF(SF,MPs)* clearly takes advantage of spatial information derived from morphological operators providing a more homogeneous result. The MP features supply a spatial regularization avoiding map pixellization effects. We remind that use MPs is different than leverage object-based image analysis (OBIA) even if the resulting maps can look similar. The MPs, derived by MM, provide new multi-scale features to enrich the pixel description while object-based classification does not provide them. In addition, in our case the unit of analysis is the pixel while in OBIA the unit is the object and the object definition is a trade-off between spatial and spectral criteria that needs to be tuned for the particular application. The second detail (Fig. 4d, 4e and 4f) depicts an agricultural zone essentially characterized by *Orchards* cultivation with large spaces of natural vegetation surrounding. Here, *RF(SF)* clearly underestimates the 5-*Orchards* class classifying the orchard land cover as 2-*Pasture and fodder* and 6-*Wooded areas*. Conversely, the *RF(SF,MPs)* approach correctly detects the pixels belonging to the 5-*Orchards* class limiting the confusion with other land cover classes. Also in this case, including spatial context via MPs allows to better discriminate among the land cover classes.

V. Conclusion

In this letter, a spatio-spectral classification framework for optical Sentinel-2 time series data was proposed and tested. The proposed approach integrates spatial information via morphological operators to enhance the discrimination among land cover classes. The obtained spatio-spectral representation was coupled with a Random Forest classifier and evaluated on two study sites. The quantitative and qualitative assessments have underlined the usefulness of the proposed approach and, more precisely, the advantage it provides in the classification of urban areas and some type of agricultural land covers. Despite the fact that mathematical morphology is a well-known tool for spatio-spectral remote sensing imagery analysis, no previous work have exploited such an approach for optical SITS classification.

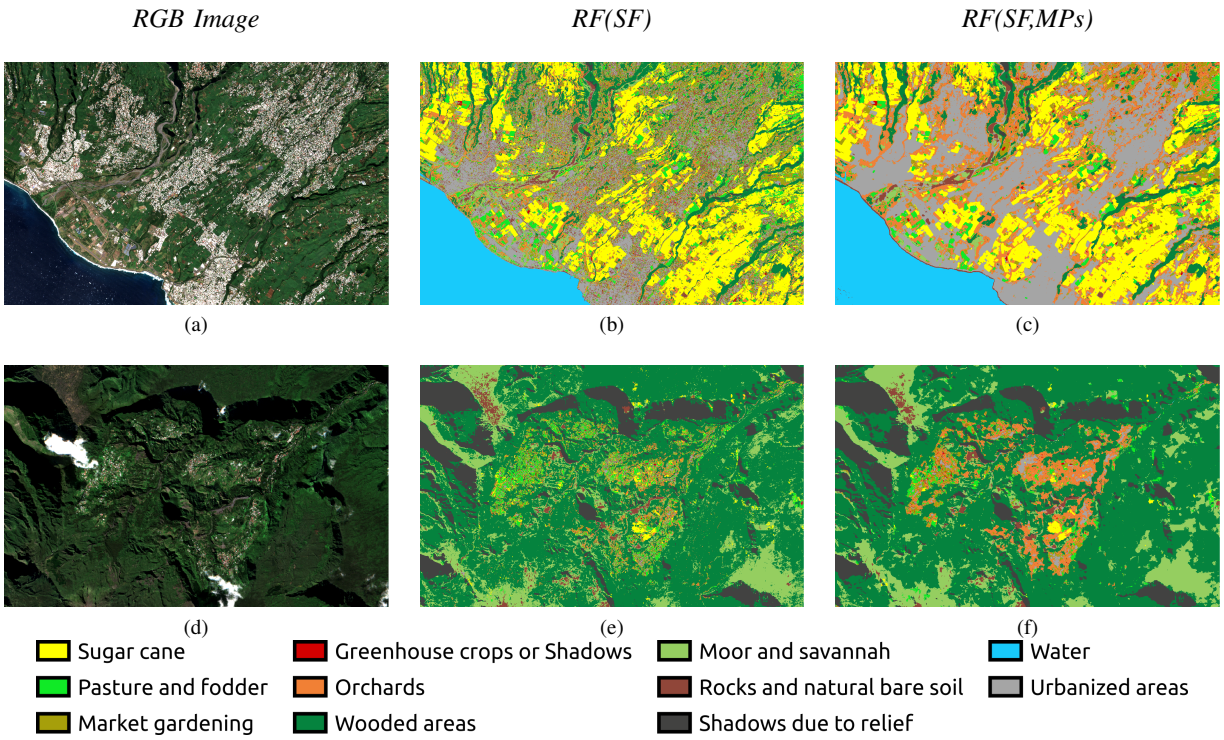

Fig. 4. Qualitative investigation of Land Cover Map details produced on the *Reunion Island* by *RF(SF)* and *RF(SF,MPs)* on two different zones (top : a mixed urban and agricultural area. Bottom: an agricultural area with natural vegetation). The RGB composite supplied as reference image is a Sentinel-2 image acquired on June 11, 2017.

VI. Acknowledgment

This work is supported by the French National Research Agency under the Investments for the Future Program, referred as ANR-16-CONV-0004 (#DigitAg) as well as from the financial contribution from the French Ministry of agriculture "Agricultural and Rural Development" trust account.

References

[1] M. Drusch, U. D. Bello, S. Carlier, O. Colin, V. Fernandez, F. Gascon, B. Hoersch, C. Isola, P. Laberinti, P. Martimort, A. Meygret, F. Spoto, O. Sy, F. Marchese, and P. Bargellini, "Sentinel-2: Esa's optical high-resolution mission for gmes operational services," *Rem. Sens. of Env.*, vol. 120, pp. 25 – 36, 2012.

[2] N. Kolecka, C. Ginzler, R. Pazur, B. Price, and P. H. Verburg, "Regional scale mapping of grassland mowing frequency with sentinel-2 time series," *Remote Sensing*, vol. 10, no. 8, p. 1221, 2018.

[3] T.-B. Ottosen, S. T. Lommen, and C. A. Skjth, "Remote sensing of cropping practice in northern italy using time-series from sentinel-2," *Comp. and Elec. in Agriculture*, vol. 157, pp. 232 – 238, 2019.

[4] E. Roteta, A. Bastarrika, M. Padilla, T. Storm, and E. Chuvieco, "Development of a Sentinel-2 burned area algorithm: Generation of a small fire database for sub-Saharan Africa," *Rem. Sens. of Env.*, vol. 222, pp. 1–17, 2019.

[5] F. Vuolo, M. Neuwirth, M. Immitzer, C. Atzberger, and W.-T. Ng, "How much does multi-temporal Sentinel-2 data improve crop type classification?" *Int. J. of Applied Earth Obs. and Geoinf.*, vol. 72, pp. 122–130, 2018.

[6] J. Inglada, A. Vincent, M. Arias, B. Tardy, D. Morin, and I. Rodes, "Operational high resolution land cover map production at the country scale using satellite image time series," *Remote Sensing*, vol. 9, no. 1, p. 95, 2017.

[7] L. Leroux, L. Congedo, B. Bellón, R. Gaetano, and A. Bégué, "Land Cover Mapping Using Sentinel-2 Images and the Semi-Automatic Classification Plugin: A Northern Burkina Faso Case Study," in *QGIS and Appl. in Agric. and Forest*. John Wiley & Sons, Inc., 2018, pp. 119–151.

[8] R. Interdonato, D. Ienco, R. Gaetano, and K. Ose, "DuPLO: A DUal view Point deep Learning architecture for time series classificatiOn," *ISPRS J. of Photogr. and Rem. Sens.*, vol. 149, pp. 91–104, 2019.

[9] D. Ienco, R. Gaetano, C. Dupaquier, and P. Maurel, "Land cover classification via multitemporal spatial data by deep recurrent neural networks," *IEEE GRSL*, vol. 14, no. 10, pp. 1685–1689, 2017.

[10] M. Fauvel, Y. Tarabalka, J. A. Benediktsson, J. Chanussot, and J. C. Tilton, "Advances in spectral-spatial classification of hyperspectral images," *Proc. of the IEEE*, vol. 101, no. 3, pp. 652–675, 2013.

[11] M. D. Mura, J. A. Benediktsson, B. Waske, and L. Bruzzone, "Morphological attribute profiles for the analysis of very high resolution images," *IEEE TGRS*, vol. 48, no. 10, pp. 3747–3762, 2010.

[12] M. Pesaresi and J. A. Benediktsson, "A new approach for the morphological segmentation of high-resolution satellite imagery," *IEEE TGRS*, vol. 39, no. 2, pp. 309–320, 2001.

[13] P. Soille and M. Pesaresi, "Advances in mathematical morphology applied to geoscience and remote sensing," *IEEE TGRS*, vol. 40, no. 9, pp. 2042–2055, 2002.

[14] M. Fauvel, J. A. Benediktsson, J. Chanussot, and J. R. Sveinsson, "Spectral and Spatial Classification of Hyperspectral Data Using SVMs and Morphological Profiles," *IEEE TGRS*, vol. 46, no. 2, pp. 3804–3814, 2008.

[15] J. W. Rouse, R. H. Haas, J. A. Schell, and D. Deering, "Monitoring the vernal advancement and retrogradation (green wave effect) of natural vegetation," *Progress Report RSC 1978-1*, p. 112, nov 1973.

[16] J. Serra, *Image Analysis and Mathematical Morphology*. Academic Press, Inc., 1983.

[17] P. Quesada-Barriuso, F. Arguello, and D. B. Heras, "Spectral–spatial classification of hyperspectral images using wavelets and extended morphological profiles," *IEEE J. of Sel. Topics in Appl. Earth Obs. and Rem. Sens.*, vol. 7, no. 4, pp. 1177–1185, 2014.

[18] J. A. Benediktsson, M. Pesaresi, and K. Arnason, "Classification and feature extraction for remote sensing images from urban areas based on morphological transformations," *IEEE TGRS*, vol. 41, pp. 1940–1949, 2003.

[19] P.-N. Tan, M. Steinbach, and V. Kumar, *Introduction to Data Mining*. Addison Wesley, 2005.